Published in final edited form as:
Breast Cancer Res Treat. 2012 August ; 134(3): 1041–1055. doi:10.1007/s10549-012-1992-x.

Strigolactones: A Novel Class of Phytohormones that Inhibit the Growth and Survival of Cancer Cells and Cancer Stem-Like Enriched Mammosphere Cells

CB Pollock[1,2], **H Koltai**[3], **Y Kapulnik**[4], **C Prandi**[5], and **RI Yarden**[1,2]

[1]Department of Health and Human Sciences, Georgetown University, 3700 Reservoir Road, NW Washington DC, 20057

[2]Lombardi Comprehensive Cancer Center Georgetown University, 3700 Reservoir Road, NW Washington DC, 20057

[3]Department of Ornamental Horticulture, Agricultural Research Organization (ARO), the Volcani Center, PO Box 6, Bet Dagan 50250, Israel

[4]Department of Field Crops and Natural Resources Institute of Plant Sciences, Agricultural Research Organization (ARO), the Volcani Center, PO Box 6, Bet Dagan 50250, Israel

[5]Department of General Chemistry and Organic Chemistry, University Turin, via P. Giuria 7, Torino 10125, Italy

Abstract

Several naturally occurring phytohormones have shown enormous potential in the prevention and treatment of several cancers. Strigolactones (SLs) are a novel class of plant hormones produced in roots and regulate new above ground shoot branching, by inhibiting self-renewal of undifferentiated meristem cells. Here we study the effects of six synthetic strigolactone analogues on breast cancer cell lines growth and survival. We show that Strigolactone analogues are able to inhibit proliferation and induce apoptosis of breast cancer cells but to a much lesser extent 'non-cancer' lines. Given the therapeutic problem of cancer recurrence which is hypothesized to be due to drug resistant cancer stem cells, we also tested the ability of Strigolactone analogues to inhibit the growth of mammosphere cultures that are typically enriched with cancer stem-like cells. We show that Strigolactones are potent inhibitors of self-renewal and survival of breast cancer cell lines grown as mammospheres and even a short exposure leads to irreversible effects on mammosphere dissociation and cell death. Immunoblot analysis revealed that SLs analogues induce activation of the stress response mediated by both P38 and JNK1/2 MAPK modules and inhibits PI3K/AKT activation. Taken together this study indicates that Strigolactones may be promising anticancer agents whose activities may be achieved through modulation of stress and survival signaling pathways.

Keywords

Plant hormone; Strigolactone; GR24; Breast cancer; Apoptosis; Proliferation; Mammosphere; Cancer stem cell; p38 MAPK; JNK1/2

Correspondence and Requests for materials should be addressed to: Ronit I. Yarden, Department of Human Science, Georgetown University, St. Mary's Hall Rm 260, Washington DC 20007. riy2@georgetown.edu Tel: 202-687-6872, Fax: 202-687-5553.

The authors declare that there is no conflict on interests.

Introduction

Breast cancer continues to be the major cause of cancer related deaths in North American women and other western countries, with an estimated 1.38 million new cancer cases diagnosed worldwide [1]. Whilst there has been a small decline in breast cancer related deaths in the past decade, it continues to be the leading cause of cancer related death in women.

An established history exists for plant derived compounds as effective anti-cancer agents [2]. Approximately 25% of drugs used in the last 20 years are derived directly from plants. Vincristine, Irinotecan, Taxanes and Camptothecins are all examples of plant-derived anti-cancer compounds. More recently a number of phytohormones have been assessed for their ability to inhibit the growth and survival of human cancer cell lines. Cytokinins are important phytohormones that regulate plant cell division and exhibit different inhibitory activities towards cancer cells [3-6]. Methyl Jasmonate (MJ) is a ubiquitous plant stress hormone belonging to the jasmonate family. MJ has been reported by numerous groups to induce apoptosis in cell lines derived from various cancer types including breast, prostate, lung, and bladder cancer [7]. MJ's mechanism of action involves disruption of Hexokinase function, resulting in severe ATP depletion and mitochondrial perturbation. The cytotoxic effects of MJ are dependent of glucose availability and involve modulation of AKT activation and generation of ROS [8-10]. Brassinosteroids (BRs) are plant steroids which regulate a number of plant processes including growth, differentiation, senescence and disease resistance. BRs have been isolated from seeds, fruits, leaves, galls and pollen. In cancer cell lines, BRs regulate Cyclin D1 and cyclin -E levels causing G1 arrest and apoptosis [11,12].

Strigolactones (SLs) are a novel class of phytohormones, so named because they contain lactone groups and were first identified as inducers of seed germination of the root parasitic plant, Striga spp. [13]. Strigolactones exert positive and negative regulation as they promotes branching of the symbiotic Arbuscular Mycorrhizal (AM) Fungi [14], induce primordial root formation [15] and inhibit shoot branching by controlling axillary meristem cells growth [16-18]. Meristem cells or root primordial cells are undifferentiated stem cells which can produce lateral organs in response to endogenous and environmental cues, while simultaneously maintaining a central pool of pluripotent stem cells [19]. Interestingly, it was shown that Strigolactones cause meristem cell cycle arrest and atrophy mainly by inhibiting cyclin B transcription ([20] and unpublished data). Currently more than ten natural SL exist and a number of synthetic analogues have been synthesized and used in plant studies [21-23]. Here we sought to examine whether SLs analogues have an inhibitory effect on human breast cancer cells, and cancer stem-like cells growth and survival. We show for the first time that SLs analogues can inhibit cancer cell proliferation and induce apoptosis (in the low micromolar range). We show that SLs analogues are potent inhibitors of mammosphere formation and cancer stem-like cell survival. In addition, SLs analogues inhibited hormone responsive and hormone independent breast cancer cell lines. Immunoblot analysis revealed that SLs analogues activated the stress induced MAPKs, P38 and JNK1/2 and inhibited PDK1 and AKT. Taken together this study indicates that SLs may be promising anticancer agents whose mechanism of action may involve stress and survival signaling modulation.

Methods

Cell culture

Cells were grown at 37 °C in a humidified 5% CO_2-95% air atmosphere. MCF-7, T47D, MDA-MB-231, MDA-436 and BJ fibroblasts (ATCC, Manassas) were maintained in

DMEM supplemented with 10% Fetal Bovine Serum (FBS). MCF-10A were maintained in DMEM supplemented with 5% horse serum (Atlanta Biologicals), 20ng/ml epidermal growth factor (EGF) (Sigma), 10μg/ml insulin (Sigma) and 500ng/ml hydrocortisone (Sigma).

Mammosphere Growth

Adherent cells were gently trypsinized, (0.05% trypsin/EDTA) washed 2× in PBS and filtered through a 40μM cell sieve to obtain a single cell suspensions. MCF7 Cells were diluted to a concentration of 10,000 cell/mL in serum-free phenol-red free MEBM (MEGM Bulletkit, Lonza) supplemented with 5 μg/ml bovine insulin, 20 ng/ml recombinant epidermal growth factor, 20 ng/ml basic fibroblast growth factor (Gibco), 1× B27 supplement, 0.5μg/ml hydrocortisone as previously described [24]. For MDA-MB-231 mammosphere cultures serum-free phenol red-free CnT-27 medium with growth additives (CellnTEC Advanced cell systems, Bern, Switzerland) was used as previously described [25]. 0.1 mL was seeded per well of a Ultralow attachment 96 well plates. The following day the indicated doses of GR-24 (ppm) or vehicle alone (0.6% acetone f/c) were added. Media was replenished every 3-4 days. Self-renewal capacity of the mammospheres was determined by re-plating and producing further generations of mammospheres. Secondary mammospheres were cultivated by dissociation (trpsinization with gently vortexing) of 10-14 day old primary mammospheres. Single cell suspensions were obtained as described above.

Strigolactone treatments

SLs analogues were solubilized in Acetone (Sigma) at stock concentrations of 1666.67 (GR24, MEB55, ST362, EGO9C) and 7500ppm (EGO5, ST357). Cells were treated at the indicated doses by diluting the hormone to the required highest concentration in the appropriate culture medium.

Crystal Violet Growth Assays

Cells were seeded at 1500 (MDA-MB-231, MDA-MB-436 and BJ fibroblasts) or 4000 cells per well of 96 well plates. The following day media was replaced with phenol-free DMEM supplemented with 10% charcoal-stripped FBS and the indicated doses of GR24, Strigolactone analogues or vehicle (acetone) alone as control. At the indicated time points, individual plates were fixed and stained with crystal violet solution (0.5% crystal violet and 25% methanol) for 15 mins, washed several times in distilled water and plates air dried overnight. Sodium citrate solution (0.1M) was used to solubilize bound crystal violet and optimal densities were measured at 560nm (Glomax® -Multi Detection plate reader, Promega).

XTT Viability Assay

Cells were seeded into a 96 well plates at 1500 cells per well (MCF10, MDA-MB-231, MDA-MB-436) or 4000 cells (MCF-7) per well in triplicate in normal growing media. The following day media was replaced with phenol-free DMEM supplemented with 10% charcoal stripped FBS and the indicated final concentrations of Strigolactone analogue or vehicle (acetone) alone. Cells were incubated for 3 days, at which time XTT (2, 3,-bis(2-methoxy-4-nitro-5-sulfophenyl)-5-[(phenylamino)-carbonyl]-2H-tetrazolium inner salt) reduction was used to quantify viability according to manufacturer's instruction (ATCC). Cells were incubated with XTT reagent for 2-3 hours at 37 °C in a humidified 5% CO_2-95% air atmosphere. Absorbance was recorded by a photometer SPEKTRAFluor Plus, Tecan (Salzburg, Austria) at 450 nm with 750 nm of reference wavelength. Cell survival was estimated from the equation: % cell survival = 100 × (At-Ac), where At and Ac are the

absorbencies (450nm) of the XTT colorimetric reaction (ATCC) in treated and control cultures respectively minus non-specific absorption measured at 750nm. Absorbance of medium alone was also deducted from specific readings.

Cell Cycle Analysis

DNA content was assessed by flow cytometry. Cells were seeded at densities of 1.5×10^5 cells (MDA-MB-231, MDA-MB-436) or 4×10^5 cells (MCF-7) per well in in 6-well plate culture dishes. The following day, the media was replaced with phenol-free DMEM supplemented with 10% charcoal-stripped FBS with the indicated concentrations of SLs analogues or vehicle alone (acetone). After 48 h, cells were washed twice with 1 × PBS (pH 7.4), centrifuged at 360g for 10 min at 4°C, and fixed in chilled ethanol (70%; v/v in PBS) with gentle vortex mixing. To determine their DNA contents, the cells were stained with 40 μg/ml propidium iodide (PI) and analyzed using a FACSCalibur flow cytometer and analyzed using CellQuest analysis software (Becton Dickinson, San Jose, CA).

Aldeflour Expression

MCF-7 mammospheres were trypsinized, gently vortexed and passed through a 40uM cell filter to produce single cell suspensions. Cells (5×10^5) were washed and resuspended in growth media (Lonza). To identify the Aldefluor-stained cell population with ALDH1 enzymatic activity, the Aldefluor kit (Stem Cell Technologies), which is designed for optimal identification and isolation of stem cells through specific interaction with human ALDH1 was used. Briefly, cells were suspended in Aldefluor assay buffer containing uncharged ALDH1-substrate, BODIPY-aminoacetaldehyde (BAAA), and incubated for 45 min at 37°C, with gently vortexing every 15 mins. BAAA is taken up by living cells through passive diffusion and then converted by intracellular ALDH into a negatively charged reaction product BODIPY-aminoacetate, which is retained inside cells expressing high levels of ALDH1, causing the cells to become brightly fluorescent. Fluorescent ALDH1-expressing cells were detected in the green fluorescence channel (520-540 nm) of a FACScan instrument (BD Biosciences). A set of cells were stained using the identical conditions with the specific ALDH inhibitor, diethylaminobenzaldehyde (DEAB), to serve as a negative control for the experiment. Propidium iodide (Sigma) fluorescence was detected using the orange fluorescence channel. Cells incubated with BAAA and DEAB were used to establish the baseline fluorescence of cells and ALDH1-positive fraction. Data were analyzed by using Cell Quest software (BD Biosciences).

Immuno-Blotting

Cell lysates were prepared using a lysis buffer containing: 50 mM Tris-HCl (pH 7.5), 125 mM NaCl, 0.5% NP-40, 0.1% SDS, 0.25% sodium deoxycholate, 1 mM EDTA, 50 mM NaF, 1 mM sodium orthovanadate, 2.5 mM sodium pyrophosphate, 1 mM sodium β-glycerophosphate, 1 mM PMSF, and a protease inhibitor cocktail (Roche Molecular Biochemicals) and cleared by centrifugation. Protein concentration was determined using the BCA Protein Assay (Pierce), and 20–50 μg of lysate were separated in a 10 or 12% SDS-PAGE gel. After wet transfer, membranes were blocked for 30 min at room temperature in 5% BSA (Sigma) in Tris-buffered saline containing 0.1% Tween-20. Primary antibody was incubated for either 1.5 hr at room temperature or overnight at 4°C. Secondary antibody was incubated for 45 min at room temperature, and proteins were visualized with West Pico Stable (Pierce). All antibodies were used at 1:1000 dilution unless otherwise stated. pT308AKT, AKT, pT180/Y182 P38MAPK, P38MAPK, pT202/Y204 ERK1/2, ERK1, pT183/Y185 pJNK1/2, pT71ATF2, pT581 MSK1, pT334 MAPKAPK, pS82 HSP27 (Cell Signaling Technology, Danvers, MA), α-tubulin (Biomarkers, 1:50,000) and horseradish peroxidase-conjugated anti-rabbit IgG and anti-mouse IgG (1:5,000, Pierce).

Statistical Analyses

Results are presented as Average ± SD of replicate analyses and are either representative of, or inclusive of at least two independent experiments. Statistical analyses were performed using student's t-test (2-tailed, paired) versus vehicle controls and regarded as being significant when $P < 0.05$ (*). Higher powers is significance ($p<0.01$, $p<0.001$) are also employed and indicated in each figure legend. IC^{50} doses for SLs were calculated by interpolation of the sigmoidal dose response curves (Graphpad Prism 4.0 software). Briefly linear regression was performed between relevant y-axis data points and interpolation calculated for x-axis unknowns.

Results

GR-24 inhibits the growth of human breast cancer cell lines

The effect of GR-24 (Supplementary Fig S1) on long-term cancer cell line growth was assessed by crystal violet assay. MCF-7 (estrogen receptor positive (ER+), tumorigenic, non-metastatic), MDA-MB-231, MDA-MB-436 (ER negative (-), metastatic) and BJ fibroblasts (normal, non-neoplastic line) were treated with GR-24 at a dose range of 0.5 to 10ppm (1.65-33μM). Growth was monitored for up to 10 days. Concentrations of 2.5-5ppm of GR-24 resulted in a significant reduction in growth compared to vehicle treated controls in MCF-7, MDA-MB-231 and MDA-MB-436. BJ fibroblasts showed no significant reduction in growth over this time period (Fig 1A). A small reduction was observed at the highest concentration (10 ppm), however this was minor when compared to the growth inhibition achieved by the same concentration of GR-24 in MCF7 and MDA-MB-231 cells. To determine the concentration of GR-24 at which 50% of long-term proliferation was inhibited (IC^{50}) after 7days, optical densities at day 7 were plotted as a percentage of vehicle controls (Fig 1B) and concentrations were calculated by interpolation. IC^{50} concentrations for MDA-MB-436, MDA-MB-231 and MCF-7 cells were 5.2ppm (17.2μM), 5.7ppm (18.8μM) and 5.7ppm (18.8μM) respectively (Fig 1B).

GR-24 induces G2/M-arrest and apoptosis

To investigate the effect of GR-24 on cell cycle progression, DNA content analyses were carried out by propidium iodide staining using flow cytometry. MCF-7, MDA-MB-231 and MDA-MB-436 cells were treated with 10, 5 and 0.5ppm concentrations of GR-24 for 48 hours and the non tumorigenic breast cell line MCF10A was used as a control. GR-24 treatment causes a dose dependent increase in the percentage of cells in G2/M phase and a concomitant decrease in the percentage of cells in G1 phase in all tumorigenic cell lines but no change was observed in the cell cycle distribution of MCF10A cells upon GR-24 treatment (Fig 2A). At higher concentrations (10ppm), GR-24 caused an increase in the sub-G1/apoptotic fraction of MDA-MB-231 (4.6 fold) and MDA-MB-436 cells (3.4 fold) compared to vehicle controls, indicating increased apoptosis. MCF-7 cells showed no change in the subG1 fraction at 10ppm (Fig 2A).

GR-24 inhibits the growth and reduces viability of breast cancer stem–like cell enriched mammosphere cultures

Tumor Initiating Cells (TICs) or Cancer Stem Cells (CSCs) are intrinsically resistant to conventional chemo- and radiation therapies [26]. These cells are able to regenerate the cellular components of the original tumor eradicated by such treatments, and ultimately lead to recurrence. The ability to target this cell population is important to develop effective treatment regimes. Mammosphere culture has been used widely for the enrichment of breast CSCs. MCF-7 cells can be propagated as ‘mammospheres’ under non-adherent, serum-free growing conditions [27,28]. To determine if GR-24 could inhibit MCF-7 mammosphere

formation, MCF-7 cells were grown as mammospheres in the presence or absence of GR-24 (Fig 3A). Mammosphere formation was completely inhibited in the presence of 2.5 –5ppm of GR-24, and severely attenuated at 1ppm, ($p<0.01$), 5 fold below the concentration required to inhibit monolayer growth (Fig 1). At 0.5ppm concentrations, growth was inhibited to a lesser degree however mammospheres were often smaller (<50uM) than vehicle treated controls ($p<0.05$). Similar results were obtained when secondary MCF-7 mammospheres were grown in the presence of GR-24 (Fig 3B). To assess the generality in mammosphere growth inhibition by GR-24, another breast cancer cells line, MDA-MB-231, was tested (Fig 3C). At 5ppm, GR-24 completely blocked MDA-MB-231 mammosphere formation. At 2.5ppm, mammopheres growth was severely attenuated, with mammospheres being substantially smaller (<50uM) compared to vehicle control groups. Importantly, the concentrations of GR-24 necessary to block MCF-7 and MDA-MB-231 mammosphere formation were 5.7 and 2.7 fold lower respectively than the IC^{50} doses for monolayer growth. Mammospheres therefore exhibit a greater sensitivity to the growth inhibitory effects of GR-24 versus monolayer culture. This is an interesting finding since mammosphere cultures reportedly are enriched with TICs and those have been shown to be inherently resistant to chemotherapy [29,30].

Effect of GR-24 on mammosphere viability and stem cells marker expression

Mammosphere viability was assessed by XTT assay (ATCC). At 5ppm, GR-24 reduced viability by approximately 80% (98.4%± 3.4 to 16.4%± 4.6) (Fig 4A). Interestingly at 2.5ppm where mammosphere formation is completely inhibited, viability remains at 68.6% ±12.4, suggesting that either timing of inhibition is critical or that apoptotic cell death cannot account solely for inhibition of mammosphere formation at this concentration. To further investigate GR-24 induced inhibition of mammosphere formation, the expression of breast stem cells markers were examined.

Aldehyde Dehydrogenase (ALDH1) has been shown to be a functional marker in the isolation of TICs in many cancer types [31,32] and MCF-7 TICs can be selected on the basis of their ALDH activity in combination with other surface markers [33]. ALDH activity was enriched in primary mammosphere relative to adherent culture and secondary mammosphere culture reached further enrichment (Fig 3B). GR-24 treatment of primary mammospheres reduced ALDH activity from 6% to 2%. This data suggests that GR-24 is a potent inhibitor of mammosphere formation and down regulation of ALDH by GR-24 may account for this activity.

Strigolactone Analogues are effective growth inhibitors of breast cancer cell lines

An additional five synthetic strigolactone (SL) analogues were obtained (Supplementary Fig S1) and tested for their ability to inhibit the growth of MCF-7 and MDA-MB-231 cells. MCF-10A cells were included as an example of a non-tumorigenic line. XTT viability assays were carried out in the presence of the indicated doses of SLs following 3 days of treatment. Resulting differences in absorbance readings following SL treatment reflect changes in proliferation and cell survival (Fig 5). IC^{50} concentrations are indicated (Table 1). Cell lines exhibited substantial variation in their response to each SL analogue, however all cancer cell lines were growth inhibited by SL treatment. ST362 and MEB55 were the most potent SLs. IC^{50} concentrations of ST362 started as low as 2.9ppm (MDA-MB-231) and for MEB55, as low as 3.9ppm (MDA-MB-231). The non-tumor cell line, MCF10A, was resistant to the effects of SL treatment up to 15ppm concentrations, with the exception of ST362, which caused a 20% reduction in viability between day 10 and 14. EGO9C was the least effective SL analogue in all cell lines tested (IC^{50} >10-15ppm). ST357 was a potent growth inhibitor of MDA-MB-231 (IC^{50}=5.0ppm) cells. Some cell lines exhibited increased XTT absorbance at lower dose concentrations. Vehicle volumes in controls were matched

with those in the highest dose only and total vehicle volumes were not matched for lower doses. Sensitivity to vehicle levels probably accounts for the suppressed viability observed in controls in relation to the lower doses in some cell lines.

To assess SL stability in aqueous solution, each SL was diluted to the desired concentration in media and stored at 4°C for 3 days, at which time the SL containing media was overlayed onto cells. After 3 days growth and viability was assessed (XTT) and results compared to cells treated with freshly diluted SL (Supplementary Fig S2). All SLs retained similar levels of activity over this time period, with the exception of EG5 which completely failed to inhibit MCF-7 growth. For this reason all SLs were diluted fresh from acetone stocks into media to desired concentrations and overlayed onto cells within 1 hour. Where necessary, media was refreshed every 3 days.

Strigolactone Analogues inhibit cell cycle progression and induce apoptosis

Here we previously showed that GR-24 treatment caused an increase in the percentage of MCF-7 and MDA-MB-231 cells in G2/M-phase and apoptosis in MDA-MB-231 and MDA-MB-436 cells. To determine whether these additional SL analogues also induced a similar mechanism of growth inhibition, cell cycle analysis was carried out. Results show a dose dependent increase in the percentage of MDA-231 and MCF7 cells in G2/M phase (Fig 6). At concentrations 25% above the IC^{50}/72h, there was evidence of increased apoptosis in MDA-MB-231 cells with increased percentages of cells in the subG1 fraction. MCF-7 cells were less sensitive to the effects of SLs at the doses tested. BJ fibroblasts were not sensitive to the effects of SLs at the doses tests (Table 2). Hoechst staining was used to analyze changes in the nucleus. ST362 treatment at 5-10 ppm resulted in increased nuclear condensation and fragmentation changes indicative of apoptosis (Fig 7A). To determine if continual SL exposure is required for growth inhibition and reduced cell survival, MDA-MB-231 cells were treated with either ST362 or MEB55 at 5ppm and 10ppm for 2, 4 and 24 hours. At each time point the SL was removed and media replaced with fresh growth media. After a total of 24 hours an XTT assay was carried out (Fig 7B). A significant decrease in viability was induced as early as 4 hours of SL treatment ($p<0.01$). No changes in cell viability were observed after 2 hours exposure. Continual exposure (24h) to each SL induced a greater reduction in cell viability ($p<0.001$) compared to 4 hours exposure. These results indicate that SL analogues induce non-reversible and time dependent decreases in cell viability.

MCF-7 Mammosphere growth is inhibited by Strigolactone treatment

Given the similar effects the other SL analogues had on breast cancer cell line growth compared to GR-24, we anticipated that the SLs would also have similar effects on MCF-7 primary mammosphere formation. As expected, all five SLs were able to completely block mammosphere formation at concentrations of 5ppm and above (Fig 8A). ST362 and MEB55 were also able to block mammosphere growth at 2.5ppm. ST357 showed a significant reduction in mammosphere growth at 2.5ppm ($p<0.01$). ST357, ST362 and MEB55 also significantly inhibited mammosphere formation at 1ppm ($p<0.01$). This data is consistent with these SLs being the most potent inhibitors of MCF-7 monolayer growth (Fig 5, Table 1). Like GR-24, the doses required to inhibit mammosphere formation were lower than that required to inhibit proliferation in monolayer cultures (5 fold lower; ST362 and MEB55, 3 fold lower; ST357). To determine if the sensitivity to SLs treatments was specific to mammosphere formation or whether it extended to the integrity and survival of mature mammospheres, MCF-7 mammospheres were grown in the absence of SLs and after 7 days (or once mammospheres had reached a mean diameter of over 100uM), SLs were added to the growth media (Fig 8) at the indicated doses. Mammospheres were monitored visually after 24 and 48hours. No changes were observed following 24 hours of SLs treatment (data

not shown). After 48 hours, mammospheres treated with ST362, ST357 and MEB55, at doses of 5 and 2.5ppm, exhibited a looser morphology and appeared to be dissociating. Representative images of mammospheres treated with 5ppm concentrations are shown (Fig 9A). Mammospheres treated with EGO9C showed a less dramatic morphological change, which correlates with the reduced potency of this SL to inhibit mammosphere formation (Fig 9). Following 5 days of treatment, mammosphere numbers (≥100μM) were counted and data presented as percentage of vehicle treated control (Fig 9B). At 5ppm concentrations EGO5, EGO9C, ST357, ST362 and MEBB55 reduced mammosphere numbers from 86.7±6.8 (vehicle control) to 23±5, 38±6.2, 6±2, 8.3±3.5 and 9.3±1.5% respectively. At 2.5ppm concentrations, mammosphere numbers were reduced to 35±6.9 (EGO5), 52±12.3 (EGO9C), 22±8.5 (ST357), 6±1.7(ST362) and 20.7±8.6 (MEB55). As expected, these results correlate closely with the analogues ability to inhibit mammosphere formation (Fig 8). XTT viability assays were also carried out on dissociated mammospheres.

Strigolactone analogues activate stress-activated MAPKs and inhibit survival signaling

To investigate the signaling mechanisms elicited by SLs in cancer cells MDA-MB-231 cells were treated with SL analogues for 1, 4 or 8 hours and lysates were analyzed by immuno-blotting. The family of MAPK enzymes plays a pivotal role in cell growth, survival and cellular stress responses. The best characterized MAPKs fall into three families, the mitogen activated extracellular signal regulated kinases (ERK1/2) which are activated in response to positive proliferation signals, c-Jun amino (N)-terminal kinases (JNK1/2/3) and p38 isoforms (p38α, β, γ, δ), both are activated by environmental stress stimuli such as DNA damage, UV irradiation and inflammatory cytokines. There was no change in the total protein levels of ERK1/2 (Fig 10A) although some dose-independent changes were noted in pERK1/2. Interestingly, ST362 induced a time dependent and dose dependent increase in pP38 levels which was first evident after 4 hours of SL exposure. At 4 hours and 8 hours, pP38 levels increased 5 fold and 13 fold respectively following ST362 treatment compared to vehicle controls (Fig 10B). To determine if pP38 levels translated into activation of down-steam signaling, nuclear P38 substrates, Activating Transcription Factor 2 (ATF2), which belongs to the ATF/cAMP response element-binding (CREB) protein family of basic region leucine zipper proteins, MSK1 (Mitogen and Stress activated protein Kinase), and heat shock protein 27, HSP27,were analyzed [34,35]. Phosphorylation of ATF2 and HSP27 was induced in response to ST362 (Fig 10A an Fig 10C). Levels were markedly increased between 4 and 8 hours after ST362 treatment and therefore followed a similar time course of activation as pP38 MAPK. There was no change in pMSK1 indicating that either p38 signaling is uncoupled from MSK1 activation or MDA-MB-231 cells already have a high basal level of pMSK1. Importantly, pT581 MSK is also a target of ERK1/2, whose phosphorylation was unchanged following SL treatment [36]. Another SL analogue, MEB55 was also able to induce phosphorylation of P38 ATF2 and HSP27 after 4 hours (Fig 10D and Fig 10F). Significant cross talk exists between P38 and JNK1/2 and both modules share subsets of MAPKKKs [37]. SL treatment also resulted in increased pJNK1/2 after 4 hours (Fig 10D).

To determine if P38 was directly responsible for the SL induced phosphorylation of ATF2 and HSP27, cells were treated with a pharmacological P38 inhibitor, SB203580. SB203580 function was confirmed by immuno-blotting for pT334 MAPKAPK, a direct P38 target [38]. pT334 MAPKAPK phosphorylation was decreased in a dose dependent manner following SB203580 exposure (Fig 10E). pT334 MAPKAPK was not increased upon MEB55 treatment, like pMSK1 (Fig 10A and Fig 10D), indicating that SLs treatment induces activation of only specific subset of P38 targets. Treatment of cells with SB203580 at concentrations of 2 μM and 10 μM was sufficient to inhibit HSP27 phosphorylation (Fig 10F) induced by ST362 and MEB55 but even 20 μM to 40 μM SB203580 did not inhibit

ATF2 phosphorylation following SL treatment (Fig 10E) and instead resulted in a dose independent increase in pATF2 levels. pP38 MAPK levels were also increased in SB203580 treated cells, a phenomenon also reported on the reagent datasheet (Cell Signaling Technology, Danvers, MA) These results show that P38 is not responsible for ATF2 phosphorylation in this system. ATF2 can also be phosphorylated on T69 and T71 directly by JNK1/2 and by Ras-ERK1/2 pathway [39]. Since ERK1/2 activation did not change upon SL exposure (Fig 10A), JNK1/2 seems the likely candidate.

The PI3K/AKT pathway regulates a wide range of cellular functions including survival and proliferation [40]. AKT activation requires phosphorylation of two critical residues, S473 near the carboxyl terminus which is considered a requirement for subsequent T308 phosphorylation and maximal AKT activation [41,42]. pT308 AKT levels decreased dramatically between 4 and 8 hours in cell treated with MEB55 and remained low at 24 hours (Fig 11). Cells treated with the less potent SL analogue, EGO5, displayed a slight delay in the inhibition of AKT phosphorylation, occurring between 8 and 24 hours. GSK3α/β activity is inhibited by phophorylation on S9 [43]. pS9/21GSK3α/β did not correlate closely with pAKT, however decreased pGSK3α/β was observed after 24 hours (Fig 10). PDK1 phosphorylates AKT on T308 [41], which is itself activated by phosphorylation on S241 [44]. Levels of pS241 PDK1 were reduced upon SL treatment and correlated closely with reduced AKT phosphorylation observed in SL treated cells (Fig 11).

Discussion

Here we have presented data showing that synthetic strigolactone, GR24, and several SL analogues possess inhibitory effects towards breast cancer cells lines growth and survival. All six analogues induced a G2/M arrest with varying degrees of apoptosis in breast cancer cells lines. Non-tumor ‘normal’ lines (MCF10A and BJ fibroblasts) displayed only limited growth inhibition and only at the highest dose ranges tested, suggesting that tumorigenic cells are more sensitive to the growth inhibitory effects of SLs and that SLs induce different responses in cancer and normal cells. Furthermore SL inhibitory effects were not limited to breast cancer cells and colon, lung and prostate cancer cells also exhibit increased sensitivity to growth inhibition effects of SL analogues (data not shown). ST362 and MEB55 induced a non-reversible reduction in cell viability after only 4 hours which correlated with phosphorylation of p38 MAPK, JNK1/2 and inhibition of AKT. p38 and JNK1/2 are stress activated MAPKs which play a crucial role in stress signaling cascade and are associated with cell cycle arrest [45] and apoptosis in some cell systems [46,47]. p38 MAPK has been reported to bind to and activate p53 and cause p53 induced apoptosis [48]. Although, SL analogues were able to induce apoptosis in cells expressing both wild-type (MCF-7) and mutant (MDA-MB-231, MDA-MB-436, T47D) p53, MCF7 cells were less sensitive. Further experiments utilizing specific inhibitors are required to determine whether SL induced apoptosis and cell cycle arrest is dependent on p38 or JNK1/2 activation. While HSP27 phosphorylation was blocked by p38 pharmacological inhibitor, it did not block the increase in ATF2 phosphorylation, which also could be activated by JNK1/2.

The differential response of cells to SL analogues (cytostatic versus cytotoxic) was dose dependent but may also be determined by cell cycle stage. The IC^{50} doses for all five SLs were 2-3 fold lower for MDA-MB-231 cells versus MCF-7 cells. This correlates with the elevated proliferation rate of the MDA-MB-231 line (S-Phase fraction, 14-18% versus 2-4% in MCF-7) and further supports a cancer therapeutic role for SLs based on their ability to target rapidly dividing cells. A better understanding of the mechanisms of action is required and may reveal ways to further sensitize cancer cells to the effects of these phytohormones. Breast cancer cells grown as ‘stem-like cell enriched’ mammospheres exhibited an increased sensitivity to SLs compared to cells grown in monolayer. SLs reduced mammosphere

growth and induced mammosphere dissociation which correlated with their ability to decrease viability. The similar effects of SLs analogues towards plant stem cells [17,18] may indicate universal mechanisms of action.

In conclusion, this is the first study to assess the effects of strigolactones, a novel class of phytohormones, on mammalian cells and particularly cancer cells. This work demonstrates that SLs may represent a new class of anti-cancer therapeutic, able to target the bulk tumor and also are effective at targeting 'cancer stem-like cells'. The mechanism of action may involve stress signaling activation and inhibition of survival signaling through inhibition of AKT.

Supplementary Material

Refer to Web version on PubMed Central for supplementary material.

Acknowledgments

We gratefully thank Drs. Rebecca Riggins, York Tomita and Michael Johnson (Lombardi Cancer Centre) for sharing reagents and helpful discussion. We thank the flow cytometry core facility at Lombardi Cancer Center for assistance with the cell cycle analysis. This work was supported by the Department of Defense Breast Program W81XWH-11-1-0190 (RIY) and by the BioBits Project, Regione Piemonte, Italy (CP).

References

1. Ferlay J, Shin HR, Bray F, Forman D, Mathers C, Parkin DM. Estimates of worldwide burden of cancer in 2008: GLOBOCAN 2008. Int J Cancer. 2010; 127:2893–917. [PubMed: 21351269]
2. Newman DJ, Cragg GM. Advanced preclinical and clinical trials of natural products and related compounds from marine sources. Curr Med Chem. 2004; 11:1693–713. [PubMed: 15279577]
3. Skoog F, Strong FM, Miller CO. Cytokinins. Science. 1965; 148:532–3. [PubMed: 17842846]
4. Ishii Y, Sakai S, Honma Y. Cytokinin-induced differentiation of human myeloid leukemia HL-60 cells is associated with the formation of nucleotides, but not with incorporation into DNA or RNA. Biochim Biophys Acta. 2003; 1643:11–24. [PubMed: 14654224]
5. Mlejnek P. Caspase inhibition and N6-benzyladenosine-induced apoptosis in HL-60 cells. J Cell Biochem. 2001; 83:678–89. [PubMed: 11746510]
6. Mlejnek P. Caspase-3 activity and carbonyl cyanide m-chlorophenylhydrazone-induced apoptosis in HL-60. Altern Lab Anim. 2001; 29:243–9. [PubMed: 11387021]
7. Cohen S, Flescher E. Methyl jasmonate: a plant stress hormone as an anti-cancer drug. Phytochemistry. 2009; 70:1600–9. [PubMed: 19660769]
8. Goldin N, Arzoine L, Heyfets A, Israelson A, Zaslavsky Z, Bravman T, Bronner V, Notcovich A, Shoshan-Barmatz V, Flescher E. Methyl jasmonate binds to and detaches mitochondria-bound hexokinase. Oncogene. 2008; 27:4636–43. [PubMed: 18408762]
9. Elia U, Flescher E. PI3K/Akt pathway activation attenuates the cytotoxic effect of methyl jasmonate toward sarcoma cells. Neoplasia. 2008; 10:1303–13. [PubMed: 18953440]
10. Oh SY, Kim JH, Park MJ, Kim SM, Yoon CS, Joo YM, Park JS, Han SI, Park HG, Kang HS. Induction of heat shock protein 72 in C6 glioma cells by methyl jasmonate through ROS-dependent heat shock factor 1 activation. Int J Mol Med. 2005; 16:833–9. [PubMed: 16211252]
11. Clouse SD, Sasse JM. BRASSINOSTEROIDS: Essential Regulators of Plant Growth and Development. Annu Rev Plant Physiol Plant Mol Biol. 1998; 49:427–451. [PubMed: 15012241]
12. Steigerova J, Oklestkova J, Levkova M, Rarova L, Kolar Z, Strnad M. Brassinosteroids cause cell cycle arrest and apoptosis of human breast cancer cells. Chem Biol Interact. 2010; 188:487–96. [PubMed: 20833159]
13. Xie X, Yoneyama K. The strigolactone story. Annu Rev Phytopathol. 2010; 48:93–117. [PubMed: 20687831]

14. Akiyama K, Ogasawara S, Ito S, Hayashi H. Structural requirements of strigolactones for hyphal branching in AM fungi. Plant Cell Physiol. 51:1104–17. [PubMed: 20418334]
15. Kapulnik Y, Delaux PM, Resnick N, Mayzlish-Gati E, Wininger S, Bhattacharya C, Sejalon-Delmas N, Combier JP, Becard G, Belausov E, Beeckman T, Dor E, Hershenhorn J, Koltai H. Strigolactones affect lateral root formation and root-hair elongation in Arabidopsis. Planta. 233:209–16. [PubMed: 21080198]
16. Rameau C. Strigolactones, a novel class of plant hormone controlling shoot branching. C R Biol. 2010; 333:344–9. [PubMed: 20371109]
17. Gomez-Roldan V, Fermas S, Brewer PB, Puech-Pages V, Dun EA, Pillot JP, Letisse F, Matusova R, Danoun S, Portais JC, Bouwmeester H, Becard G, Beveridge CA, Rameau C, Rochange SF. Strigolactone inhibition of shoot branching. Nature. 2008; 455:189–94. [PubMed: 18690209]
18. Umehara M, Hanada A, Yoshida S, Akiyama K, Arite T, Takeda-Kamiya N, Magome H, Kamiya Y, Shirasu K, Yoneyama K, Kyozuka J, Yamaguchi S. Inhibition of shoot branching by new terpenoid plant hormones. Nature. 2008; 455:195–200. [PubMed: 18690207]
19. Sharma VK, Fletcher JC. Maintenance of shoot and floral meristem cell proliferation and fate. Plant Physiol. 2002; 129:31–9. [PubMed: 12011335]
20. koltai H, Dor E, Hershenhorn J, Daniel M, Weininger S, Lekalla S, Shealtiel H, Bhattacharya C, Eliahu E, Resnick N, Barg R, Kapulnik Y. Strigolactones' Effect on Root Growth and Root-Hair Elongation May Be Mediated by Auxin-Efflux Carriers. Journal of Plant Growth Regulation. 2010; 29:129–136.
21. Dor E, Joel DM, Kapulnik Y, Koltai H, Hershenhorn J. The synthetic strigolactone GR24 influences the growth pattern of phytopathogenic fungi. Planta. 2011; 234:419–27. [PubMed: 21688170]
22. Bhattacharya C, Bonfante P, Deagostino A, Kapulnik Y, Larini P, Occhiato EG, Prandi C, Venturello P. A new class of conjugated strigolactone analogues with fluorescent properties: synthesis and biological activity. Org Biomol Chem. 2009; 7:3413–20. [PubMed: 19675895]
23. Mwakaboko AS, Zwanenburg B. Single step synthesis of strigolactone analogues from cyclic keto enols, germination stimulants for seeds of parasitic weeds. Bioorg Med Chem. 2011; 19:5006–11. [PubMed: 21757362]
24. Dontu G, Abdallah WM, Foley JM, Jackson KW, Clarke MF, Kawamura MJ, Wicha MS. In vitro propagation and transcriptional profiling of human mammary stem/progenitor cells. Genes Dev. 2003; 17:1253–70. [PubMed: 12756227]
25. Prud'homme GJ, Glinka Y, Toulina A, Ace O, Subramaniam V, Jothy S. Breast cancer stem-like cells are inhibited by a non-toxic aryl hydrocarbon receptor agonist. PLoS One. 5:e13831. [PubMed: 21072210]
26. Singh A, Settleman J. EMT, cancer stem cells and drug resistance: an emerging axis of evil in the war on cancer. Oncogene. 29:4741–51. [PubMed: 20531305]
27. Charafe-Jauffret E, Ginestier C, Iovino F, Wicinski J, Cervera N, Finetti P, Hur MH, Diebel ME, Monville F, Dutcher J, Brown M, Viens P, Xerri L, Bertucci F, Stassi G, Dontu G, Birnbaum D, Wicha MS. Breast cancer cell lines contain functional cancer stem cells with metastatic capacity and a distinct molecular signature. Cancer Res. 2009; 69:1302–13. [PubMed: 19190339]
28. Cariati M, Naderi A, Brown JP, Smalley MJ, Pinder SE, Caldas C, Purushotham AD. Alpha-6 integrin is necessary for the tumourigenicity of a stem cell-like subpopulation within the MCF7 breast cancer cell line. Int J Cancer. 2008; 122:298–304. [PubMed: 17935134]
29. Li X, Lewis MT, Huang J, Gutierrez C, Osborne CK, Wu MF, Hilsenbeck SG, Pavlick A, Zhang X, Chamness GC, Wong H, Rosen J, Chang JC. Intrinsic resistance of tumorigenic breast cancer cells to chemotherapy. J Natl Cancer Inst. 2008; 100:672–9. [PubMed: 18445819]
30. Singh A, Settleman J. EMT, cancer stem cells and drug resistance: an emerging axis of evil in the war on cancer. Oncogene. 2010; 29:4741–51. [PubMed: 20531305]
31. Jiang F, Qiu Q, Khanna A, Todd NW, Deepak J, Xing L, Wang H, Liu Z, Su Y, Stass SA, Katz RL. Aldehyde dehydrogenase 1 is a tumor stem cell-associated marker in lung cancer. Mol Cancer Res. 2009; 7:330–8. [PubMed: 19276181]

32. Burger PE, Gupta R, Xiong X, Ontiveros CS, Salm SN, Moscatelli D, Wilson EL. High aldehyde dehydrogenase activity: a novel functional marker of murine prostate stem/progenitor cells. Stem Cells. 2009; 27:2220–8. [PubMed: 19544409]
33. Croker AK, Goodale D, Chu J, Postenka C, Hedley BD, Hess DA, Allan AL. High aldehyde dehydrogenase and expression of cancer stem cell markers selects for breast cancer cells with enhanced malignant and metastatic ability. J Cell Mol Med. 2009; 13:2236–52. [PubMed: 18681906]
34. Cuadrado A, Nebreda AR. Mechanisms and functions of p38 MAPK signalling. Biochem J. 2010; 429:403–17. [PubMed: 20626350]
35. Saccani S, Pantano S, Natoli G. p38-Dependent marking of inflammatory genes for increased NF-kappa B recruitment. Nat Immunol. 2002; 3:69–75. [PubMed: 11743587]
36. Deak M, Clifton AD, Lucocq LM, Alessi DR. Mitogen- and stress-activated protein kinase-1 (MSK1) is directly activated by MAPK and SAPK2/p38, and may mediate activation of CREB. Embo J. 1998; 17:4426–41. [PubMed: 9687510]
37. Cargnello M, Roux PP. Activation and function of the MAPKs and their substrates, the MAPK-activated protein kinases. Microbiol Mol Biol Rev. 75:50–83. [PubMed: 21372320]
38. Gum RJ, Young PR. Identification of two distinct regions of p38 MAPK required for substrate binding and phosphorylation. Biochem Biophys Res Commun. 1999; 266:284–9. [PubMed: 10581204]
39. Bhoumik A, Lopez-Bergami P, Ronai Z. ATF2 on the double - activating transcription factor and DNA damage response protein. Pigment Cell Res. 2007; 20:498–506. [PubMed: 17935492]
40. Gong G, Stern HS, Cheng SC, Fong N, Mordeson J, Deng HW, Recker RR. The association of bone mineral density with vitamin D receptor gene polymorphisms. Osteoporos Int. 1999; 9:55–64. [PubMed: 10367030]
41. Woodgett JR. Recent advances in the protein kinase B signaling pathway. Curr Opin Cell Biol. 2005; 17:150–7. [PubMed: 15780591]
42. Scheid MP, Marignani PA, Woodgett JR. Multiple phosphoinositide 3-kinase-dependent steps in activation of protein kinase B. Mol Cell Biol. 2002; 22:6247–60. [PubMed: 12167717]
43. Shaw M, Cohen P, Alessi DR. Further evidence that the inhibition of glycogen synthase kinase-3beta by IGF-1 is mediated by PDK1/PKB-induced phosphorylation of Ser-9 and not by dephosphorylation of Tyr-216. FEBS Lett. 1997; 416:307–11. [PubMed: 9373175]
44. Casamayor A, Morrice NA, Alessi DR. Phosphorylation of Ser-241 is essential for the activity of 3-phosphoinositide-dependent protein kinase-1: identification of five sites of phosphorylation in vivo. Biochem J. 1999; 342(Pt 2):287–92. [PubMed: 10455013]
45. Correze C, Blondeau JP, Pomerance M. p38 mitogen-activated protein kinase contributes to cell cycle regulation by cAMP in FRTL-5 thyroid cells. Eur J Endocrinol. 2005; 153:123–33. [PubMed: 15994754]
46. Iyoda K, Sasaki Y, Horimoto M, Toyama T, Yakushijin T, Sakakibara M, Takehara T, Fujimoto J, Hori M, Wands JR, Hayashi N. Involvement of the p38 mitogen-activated protein kinase cascade in hepatocellular carcinoma. Cancer. 2003; 97:3017–26. [PubMed: 12784337]
47. Chang HL, Wu YC, Su JH, Yeh YT, Yuan SS. Protoapigenone, a novel flavonoid, induces apoptosis in human prostate cancer cells through activation of p38 mitogen-activated protein kinase and c-Jun NH2-terminal kinase 1/2. J Pharmacol Exp Ther. 2008; 325:841–9. [PubMed: 18337475]
48. She QB, Chen N, Dong Z. ERKs and p38 kinase phosphorylate p53 protein at serine 15 in response to UV radiation. J Biol Chem. 2000; 275:20444–9. [PubMed: 10781582]

Abbreviations

SL	Strigolactone
CSC	Cancer stem cell
Ppm	parts per million

PI	Propidium iodide
ERK	Extracellular regulated kinase
P38 MAPK	P38 Mitogen-activated protein kinase
MSK1	Mitogen- and stress-activated protein kinase
ATF2	Activating transcription factor 2
AKT	Protein kinase B
IC	Inhibitory concentration

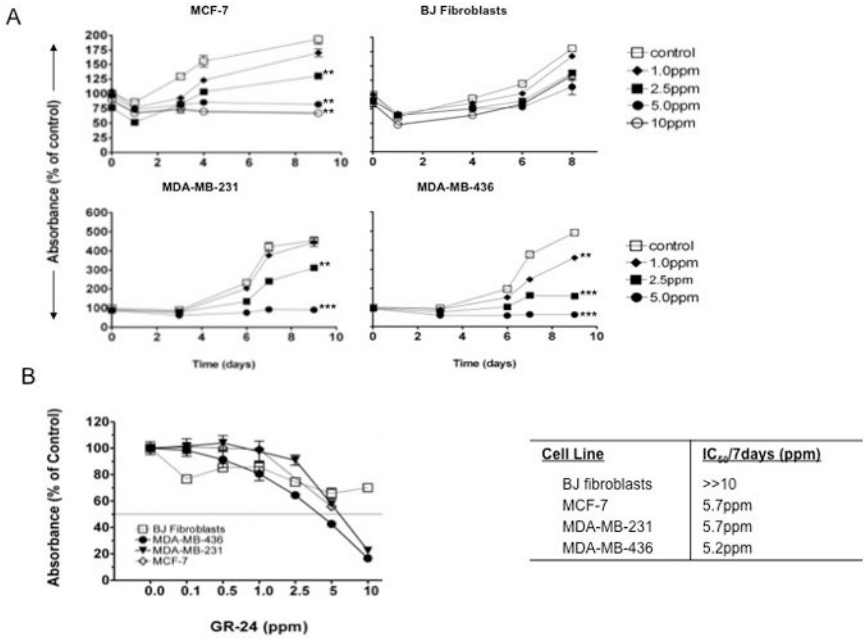

Cell Line	IC_{50}/7days (ppm)
BJ fibroblasts	>>10
MCF-7	5.7ppm
MDA-MB-231	5.7ppm
MDA-MB-436	5.2ppm

Fig 1.

Effect of GR-24 on breast cancer cell line proliferation. MDA-MB-231, MDA-MB-436, MCF-7 and BJ 'normal' fibroblasts were exposed to varying concentrations of GR-24 for up to 10 days. At the indicated time points, plates were stained with crystal violet. Data are reported as the Percent Absorbance (560nm) of vehicle control. Average ± standard deviations (SD). Student's t-test (2-tailed, paired) was used to evaluate GR-24 treated groups with vehicle (control) groups at final time point and regarded as being significant if $p < 0.05$ (*), very significant if $p<0.01$ (**), extremely significant if $p<0.001$ (***). (**B**) Graph showing the light absorbance reading (560nm) after 7 days exposure to the indicated doses of GR-24. Data expressed as a percentage of vehicle controls. Average of triplicate samples ± SD. Horizontal line (---) marks 50% reduction in Absorbance (560nm) relative to vehicle controls. Right, Table showing inhibitory concentrations required for 50% reduction in growth after 7days (IC50/72d), and calculated by performing linear regression with interpolation between relevant y-axis data points (GraphPad Prism Software).

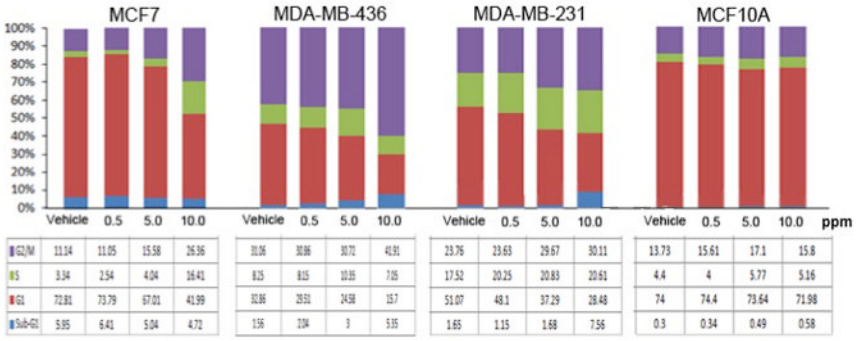

Fig 2.

: Effect of GR-24 on cell cycle progression. Cell Cycle Analysis of cell lines treated with the SL analogue, GR-24 was carried out by propidium Iodide staining and Flow cytometry analysis of total DNA content to evaluate the number of cells in different phases of the cell cycle, including subG_1 peak detection following Strigolactone treatment. Cells were treated with the indicated doses of GR-24 for 48 hours. Data is representative of two independent experiments.

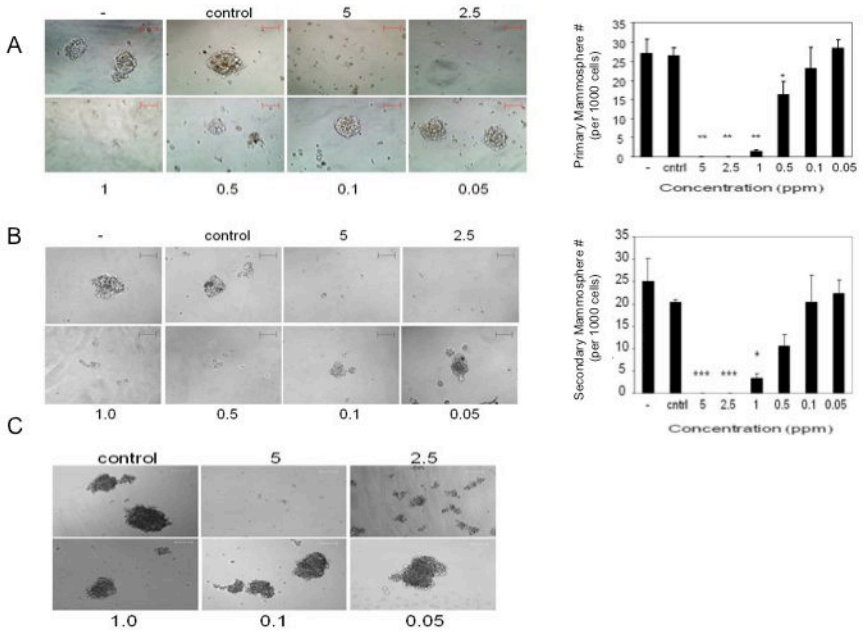

Fig 3.

Mammosphere formation in the presence of GR-24. Images representative bright field images of either primary mammospheres (A) or secondary mammospheres (B) or MDA-MB-231 primary mammospheres (C) grown in the presence of the indicated doses of GR-24, vehicle control or untreated (-). Magnification: 10× (A, B), 20× (C), scale bar 100uM. Bar graphs, showing the average number of mammospheres (over 100uM diameter) per well of 96 well plate, visualized at 5× magnification. Data reported as average ± standard deviations (SD) of triplicate wells and representative of at least two independent experiments. Student's t-test (2-tailed, paired) was used to evaluate GR-24 treated groups with vehicle (control) group and regarded as being significant if $p < 0.05$ (*), very significant if $p<0.01$ (**), extremely significant if $p<0.001$ (***).

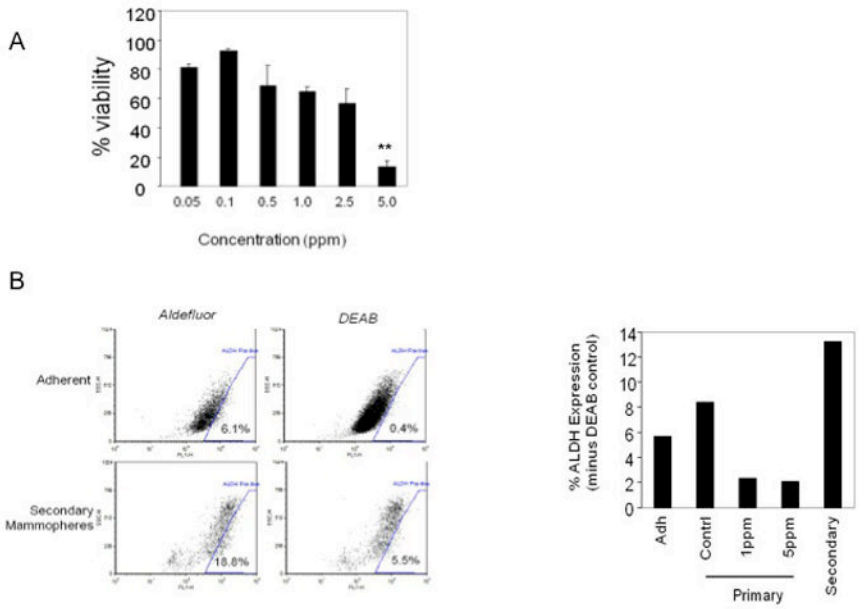

Fig 4.

Viability and ALDH expression following GR-24 treatment. (A) XTT viability assay on MCF-7 secondary mammospheres treated with GR-24. GR-24 was added at the indicated final concentrations. 5 days later, cell viability was determined (XTT kit, ATCC). Data reported as % of vehicle control. Bars, Average ± standard deviations (SD) of triplicate samples. Student's t-test (2-tailed, paired) was used to evaluate 5ppm treated group with control group, p=0.0065 (**), (**B**) Analysis of ALDH1 expression in secondary MCF-7 mammospheres. Adherent MCF-7 cells and 8 days old secondary mammospheres were prepared as single cells suspensions and ALDH expression was analyzed according to manufacturer's instructions (Aldefluor kit, Stem Cell Technologies, Vancouver, CA). Right, Bar graph showing the percentage of ALDH positive cells in either adherent MCF-7 cultures, primary (Adh), primary mammospheres grown in the presence of either 5ppm, 1ppm GR24 or vehicle (contrl) alone (0.6% Acetone) and 8 day old secondary mammospheres (secondary). Secondary mammospheres exhibit an 2.4 fold enrichment for ALDH activity. Primary mammospheres exhibit an small increase of 6% to 8% positivity for ALDH expression. GR-24 treatment causes a reduction in ALDH expression from 6% to 2%.

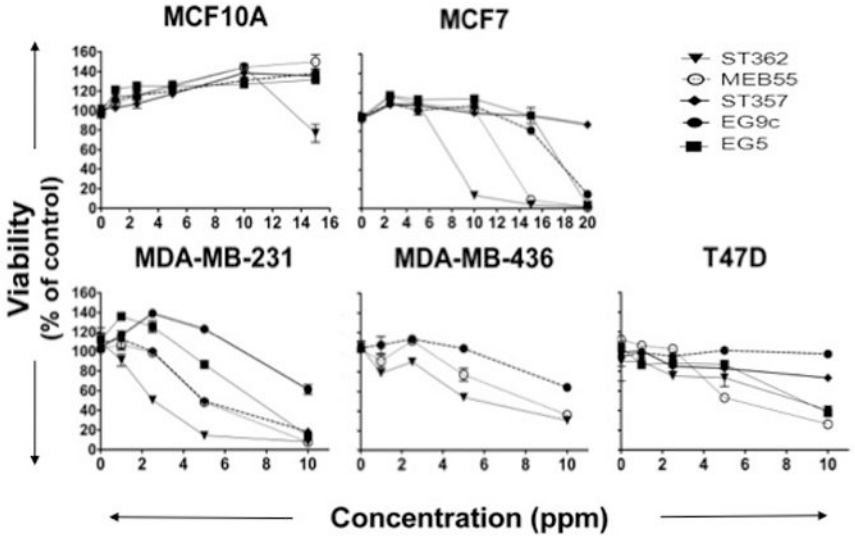

Fig 5.

Effect of Strigolactone analogues on human cancer cell line growth and viability. Cells were seeded into 96 well plates in normal growing media. The following day media was replaced with phenol free DMEM supplemented with 10% charcoal stripped serum and the indicated doses of Strigolactone Analogue or vehicle (control) alone. Viability was assayed after 3 days (XTT, ATCC). Graphs are representative of two independent experiments with duplicate replicate wells for each analysis.

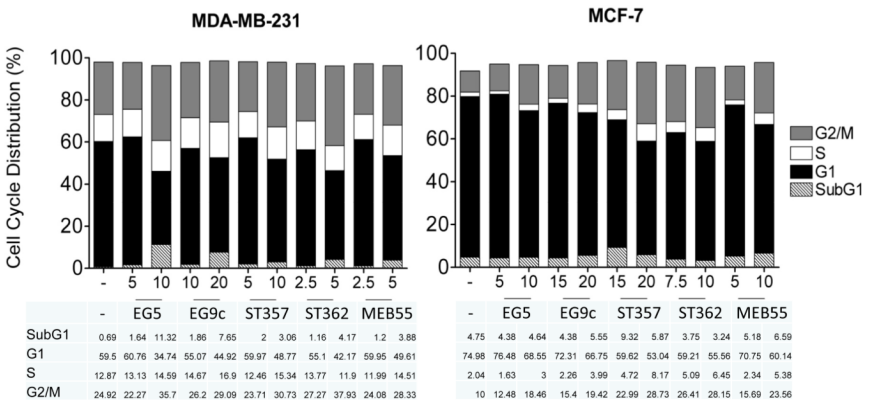

Fig 6.

Cell Cycle Analysis of cancer cell lines treated with SL Analogues. Cells were treated for 48 hours with two different concentrations of SL analogue in phenol free- DMEM supplemented with 10% charcoal stripped serum and Strigolactone at either IC_{50}/72h or ~IC50/72h+25% concentrations. (MCF-7 cells were IC^{50}/72h >10ppm, so 20ppm concentrations were used. Where IC50/72h=ND, concentrations were selected arbitrarily). SL Analogues increase the percentage of cells in G2 phase in both MDA-MB-231 and MCF-7 cells. MDA-MB-231 cells exhibit increased subG1/apoptotic fractions at higher concentrations, as did ST357 in MCF-7 cells.

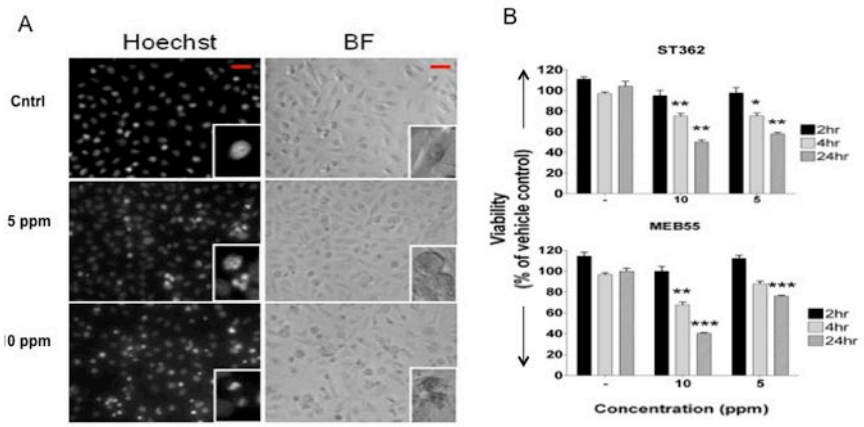

Fig 7.

Strigolactone analogues induce apoptosis in MDA-MB-231 cells (A) Hoechst33342 staining of MDA-MB-231 cells treated with the indicatated doses of the Strigolacone analogue ST362. Cells were treated with the indicated doses of SLs for 24 hours. Cells were fixed in 1% paraformaldehyde and stained with Hoechst33342. Magnification 200×. Scale bar, 50uM. Evidence of cell shrinkage, nuclear condensation and nuclear fragmentation is observed, as well as eccentric nuclei, (insert). (B) XTT viability assay following SL exposure. MDA-MB-231 cells were treated with the indicated concentrations of SL. After 2, 4 or 24 hours media was removed, cells were washed and media was replaced with growth media minus SL. Cell viability was assessed at 24hrs. ST362 and MEB55 induce a non-reversible reduction in cell viability in a dose-dependent and incubation time dependent manner. Data are reported as % of vehicle control groups. Bars represent Average ± standard deviations (SD). Statistical analysis, student's t-test (2-tailed, paired) versus vehicle controls and regarded as being significant if $p < 0.05$ (*), $p<0.01$ (**), $p<0.001$ (***).

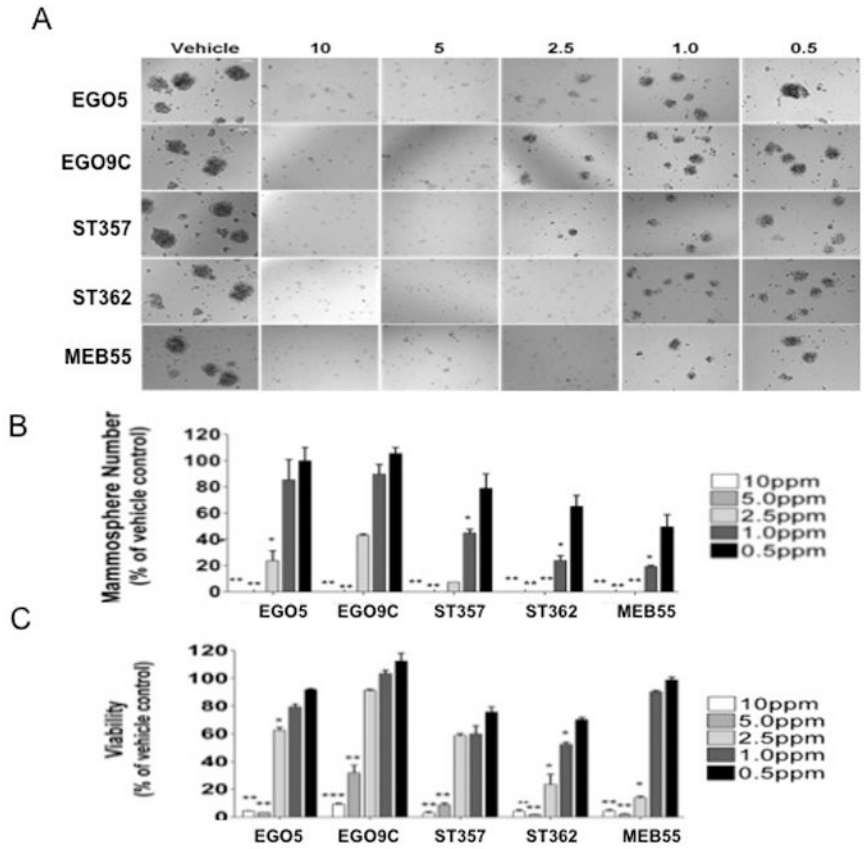

Fig 8.

Effect of SLs on MCF-7 mammosphere formation. MCF7 cells were seeded in MEBM media into low attachment, 96 well plates in duplicate at 3000 cells per well. The same day the indicated doses of Strigolactone analogues were added. After 7 days representative images were taken (A), mammospheres numbers over 100uM diameter were counted (B). Statistical analysis was done by two tail student t-test $p \leq 0.05$ (*), $p \leq 0.005$ (**), $p \leq 0.001$ (***).

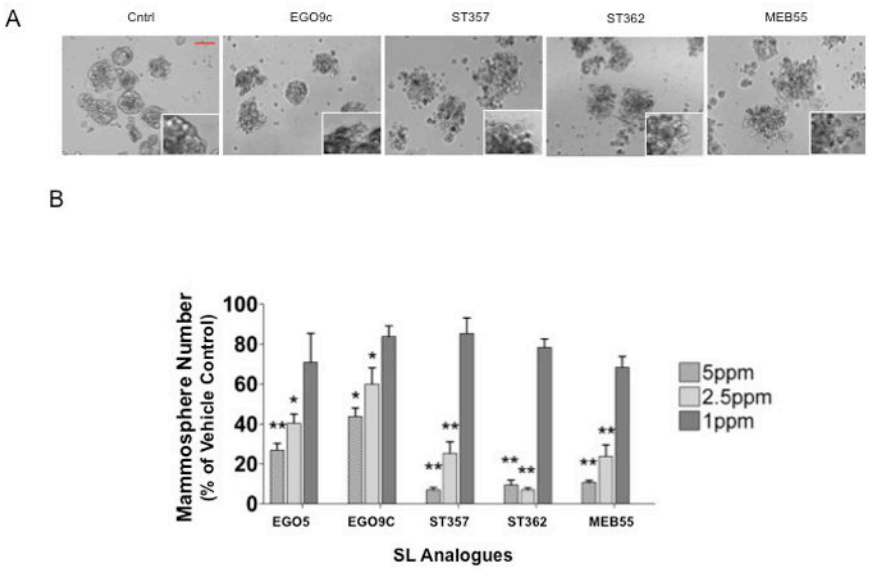

Fig 9.

Effect of SLs on primary MCF-7 mammosphere integrity and viability. MCF7 cells were seeded in MEBM media into low attachment, 96 well plates in duplicate at 3000 cells per well and primary mammospheres left to grow for 7 days. At which time the indicated doses of Strigolactone analogues were added to the media. (A) Representative images were taken of mammospheres after 2 days of Strigolactone treatment. Dissociation is evident after 2 days exposure to SLs. Magnification 100×, Scale bar, 100uM. Insert, zoomed image. (B) Mammospheres numbers (>100μM) following 5 days Strigolactone treatment. Statistical Analysis, two tailed students t-test, p≤0.05 (*), p≤ 0.01 (**), p≤0.001 (***)

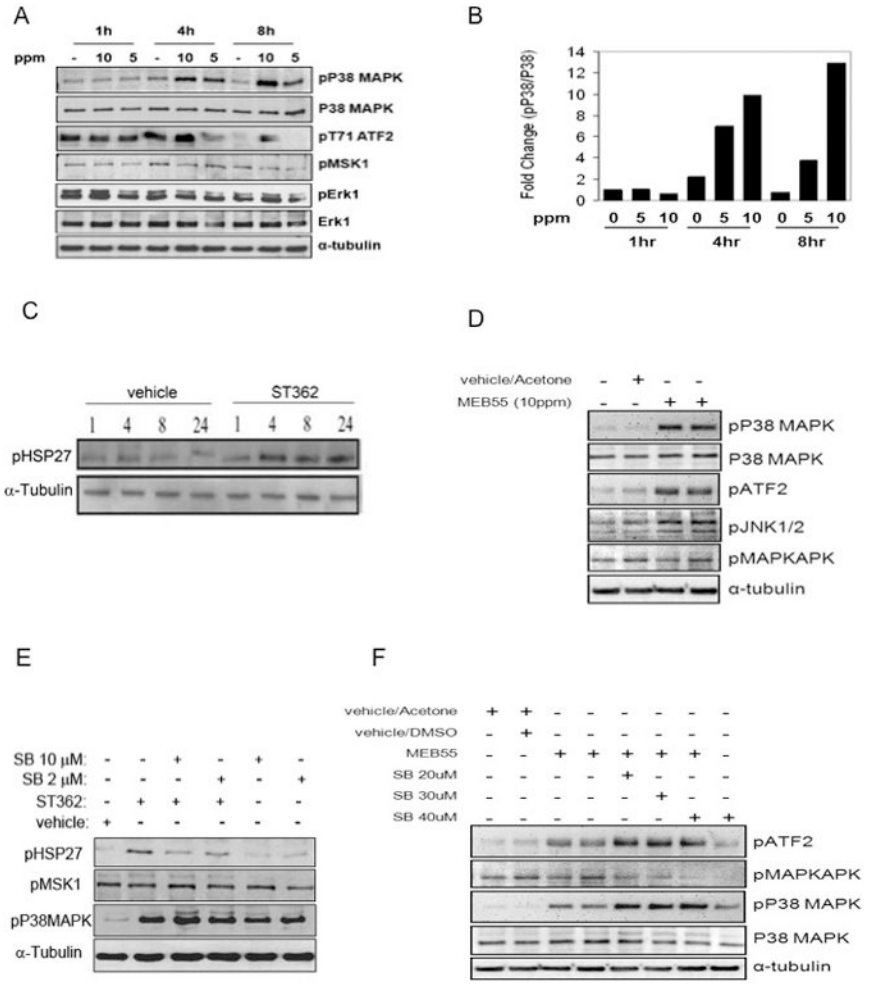

Fig 10.

SLs analogues induce stress response. Immunoblot analysis of MDA-MB-231 cells treated with SL analogues. (A) immunoblot analysis of cells following treatment with ST362 at either 10 or 5 ppm concentration or vehicle alone (-) for the indicated time points. (B) Bar graph showing densitometric quantification of pP38 levels as shown in (A). (C) Immunoblot analysis of cells treated with either vehicle or ST362 (10 ppm) for 1, 4,8 and 24 hrs. Phosophorylation of HSP27 was analyzed. (D) MDA-MB-231 cells were treated with 10 ppm of the Strigolactone analogue, MEB55, or vehicle only for 4 hrs and then harvested and analyzed by SDS-PAGE for protein expression. Levels of the indicated proteins are depicted. (E) Immunoblot analysis of cells treated with ST362 alone or together with the indicated concentrations of SB203580. (F) Immunoblot analysis of cells treated with MEBB55 alone or together with SB203580. Cells were pretreated with SB203580 for 1hour prior to addition of ST362 or MEB55. Cells were treated with ST362 or MEB55 alone or together with SB203580 for 4 hours.

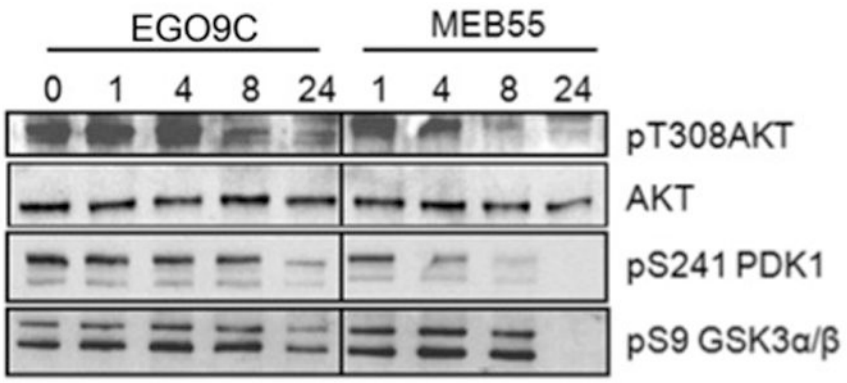

Fig 11.

SLs analogues inhibit survival signaling. Immunoblot analysis of MDA-MB-231 cells treated with either vehicle alone or with 10 ppm of either EGO5 or MEB55 for 1,4,8, 24hrs. Whole cell extracts were prepared and analyzed for the expression of the indicated proteins.

Table 1

IC^{50} Concentrations of SL analogues in cancer cells lines

Tumor Cell Lines	IC_{50} (ppm) at 72hours				
	EGO5	EGO9C	ST357	ST362	MEB55
Breast					
MCF10A	>15	>15	>15	>15	>15
MCF-7	17.5	17.3	>20	8.1	>12.8
T47D	8.8	>10	>10	8.6	5.0
MDA-MB-231	7.5	>10	5.0	2.9	3.9
MDA-MB-436	ND	>10	ND	5.9	8.3

Table 2

Cell Cycle Analysis of cell lines treated with SL analogues

Cell Line	SL (dose/ppm)	SubG1/poptosis	Cell Cycle Distribution (%)		
			G1	S	G2
BJ fibroblast	Vehicle	0.21	84.25	2.510	10.17
	EGO5 (10)	0.49	82.29	4.480	10.50
	ST362 (5)	0.72	83.42	1.580	12.86
	MEB55 (5)	0.57	78.96	5.930	11.54
MDA-MB-231	Vehicle	0.41	60.43	13.02	24.08
	EGO5 (10)	11.32	34.74	14.59	35.70
	ST362 (5)	4.17	42.17	11.90	37.93
	MEB55 (5)	3.88	49.61	14.51	28.33